

Polymorphism-dependent fluorescence of 9,10-bis(pentafluorobenzoyloxy)anthracene

Shigeo Kohmoto,^{a,*} Ryota Tsuyuki,^a Hyuma Masu,^b Isao Azumaya^b
and Keiki Kishikawa^a

^a*Department of Applied Chemistry and Biotechnology, Graduate School of Engineering,
Chiba University, 1-33 Yayoi-cho, Inage-ku, Chiba 263-8522, Japan*

^b*Faculty of Pharmaceutical Sciences at Kagawa Campus, Tokushima Bunri University,
1314-1 Shido, Sanuki, Kagawa 769-2193, Japan*

Received 14 September 2007; revised 1 November 2007; accepted 5 November 2007
Available online 7 November 2007

Abstract—Anthracene derivatives possessing pentafluorobenzoyloxy moieties at 9- and 10-positions showed polymorphism affording two types of fluorescent crystals with blue and bluish green fluorescence in their crystalline state, respectively. Their single crystal X-ray structures showed that the degree of overlap of anthracene moieties was responsible for the difference in fluorescence. Fluorescence in the crystalline state originated in the dimer emission deduced from their excitation spectra.

© 2007 Elsevier Ltd. All rights reserved.

The manipulation of weak interactions is the key protocol for designing of novel functional materials in crystal engineering.¹ The choice of proper interactions settles a specific conformation or geometrical arrangement of molecules in the crystal lattice, which leads to characteristic properties originated in their particular packing structure. We have been interested in the fluorescence tuning of aromatic compounds in the crystalline state.² Weak intermolecular interactions such as CH/ π ,³ halogen/ π ,⁴ and π - π ⁵ interactions are playing important roles there. Hydrophobic interaction is also important. Recently, the intensity tunable solid-state fluorescence is reported based on the effect of alkyl chain packing of anthracene-2,6-disulfonic acid amine salts.⁶ Not only the intensity of the emission but also its tone can be tuned by the subtle differences in the packing of aromatic fluorophores. It was shown that molecular arrangement of aromatic fluorophores could be modified by inclusion of guest molecules resulting in the slight shift in excimer emission.⁷ The degree of the overlap of aromatic fluorophores could be reflected in their fluorescence. This type of fluorescence tuning can be attained by applying the morphologically different crystals of aromatic fluorophores. But the example of this poly-

morphism-dependent fluorescence is very limited.⁸ In this Letter, we report on the novel example of the polymorphism-dependent fluorescence and the crystalline-state dimer emission of anthracene-based crystals. The key intermolecular interaction in our study is the CF $\cdots\pi$ _F interaction. Two anthracene derivatives **1**⁹ and **2**,¹⁰ possessing pentafluorophenyl and phenyl groups, respectively, were prepared. Compound **1** showed polymorphism affording two types of crystals depending on the way of recrystallization. Recrystallization from ethyl acetate gave the blue fluorescent crystals (B-form) as pale yellow plates.

Recrystallization from ethyl acetate pervaded with hexane vapor yielded bluish green fluorescent crystals (BG-form) as fine yellow needles with a width of 20–50 μ m. Their solid-state fluorescence spectra are shown in Figure 1 together with the photographs of the B-form and the BG-form irradiated with 366 nm light. In CHCl₃ solution, both **1** (the B- and BG-forms) and **2** showed identical shape of fluorescence spectra with vibronic bands typical to those of anthracene. Fluorescence spectrum of the B-form in the crystalline state was almost identical to that of **2** in the crystalline state with the emission maximum (λ_{max}) at 458 nm. In contrast, the red-shifted fluorescence was observed for the BG-form (λ_{max} 485 nm) in the crystalline state. It is known that excimer emission wavelength of anthracene depends on

* Corresponding author. Tel.: +81 43 290 3420; fax: +81 43 290 3422; e-mail: kohmoto@faculty.chiba-u.jp

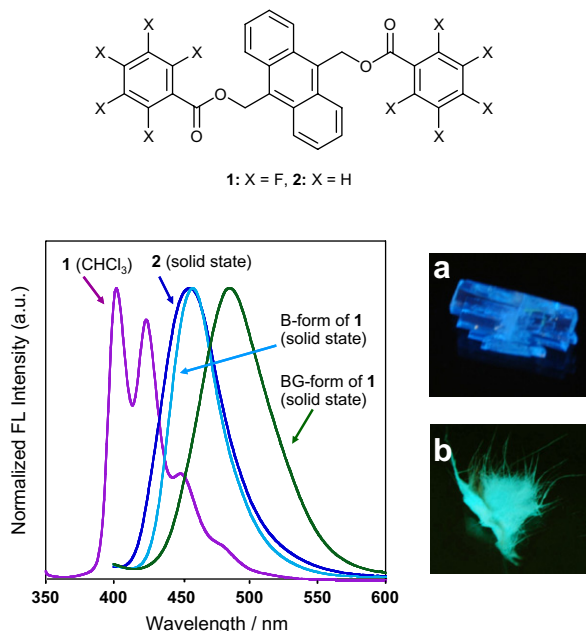


Figure 1. Fluorescence spectra of **1** and **2** at ambient temperature. Violet, blue, sky blue, and green lines show those of **1** in CHCl_3 (5.0 μM), **2** in the solid state, the B-form of **1** in the solid state, and the BG-form of **1** in the solid state, respectively, excited at 339 nm. Photographs (a) and (b) show fluorescence of the crystals of the B-form (plates) and the BG-form (fine needles) of **1**, respectively, irradiated with 366 nm light.

the degree of the overlap of anthracene π -planes.¹¹ Therefore, it is expected that the B-form and **2** have the similar overlapping pattern of anthracene moieties while the BG-form has more efficient overlapping of them. It is noteworthy to mention that anthracene excimer emission at room temperature is rare relative to that of other polycyclic aromatic compounds owing to their efficient photodimerization and anthracene itself shows only the monomer emission in the crystalline state.^{7,12} We tried to prepare amorphous samples of the B- and BG forms of **1** and **2**, in which the molecules are packed in a random fashion, by melting followed by rapid cooling or evaporation of the solvent from their solution samples. The fluorescence spectra obtained were slightly different depending on the trial. For the B- and BG forms and **2**, their λ_{max} thus obtained were in the range of 439–453 nm, which is slightly shorter than those of the fluorescence spectra of the B-form and **2** in the crystalline state. Probably, the samples prepared by the above-mentioned treatment were not amorphous but they might be disordered microcrystals judging from the λ_{max} values.

To confirm that the differences in their fluorescence originate in the degree of the overlap of anthracene moieties, the single crystal X-ray structure analysis of **1** (the B-form and the BG-form) and **2** was carried out. A reasonable overlap of anthracene moieties was observed for the BG-form while they were more apart in the B-form and in **2** (Fig. 2). Figure 2a and b shows the packing diagram of the B- and BG-forms, respectively. In both forms, the anthracene moieties are partly stacked to form columnar

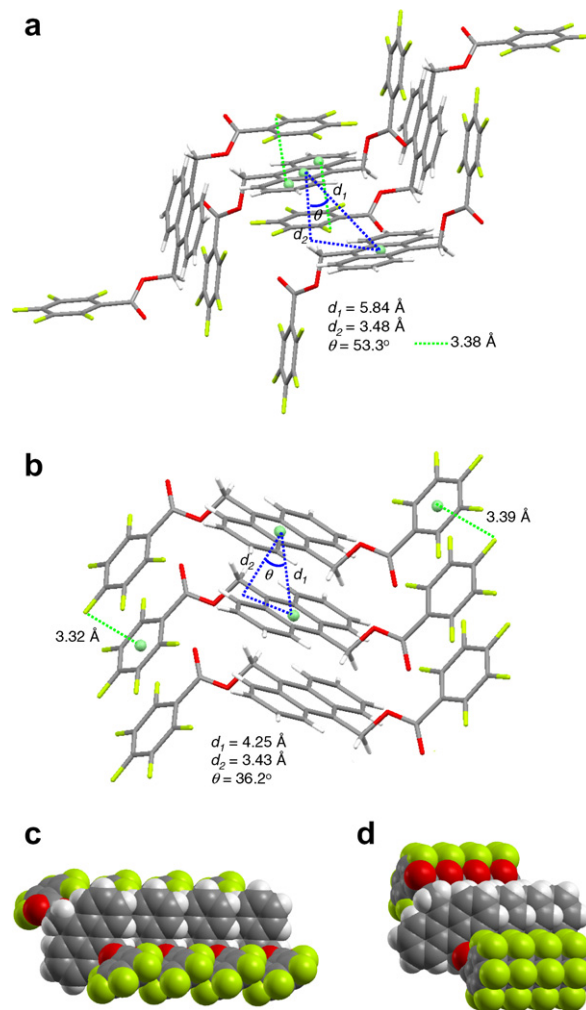


Figure 2. Single crystal X-ray structure of the B-form (a) and the BG-form (b) of **1**. Space-fill presentations of the stacking of anthracene moieties in the B-form (c) and in the BG-form (d) to show the difference in the degree of the overlap of anthracene moieties.

structures. Figure 2c and d shows the space-fill presentations of their columns, respectively. In the B-form, the distance between the centroids of anthracene moieties (d_1) is 5.84 Å and the slipping angle (θ) created by the disposition of centroids is 53.3°. In contrast to this, the corresponding distance and angle are 4.25 Å and 36.2° in the BG-form, respectively, which indicates a better overlapping of the anthracene moieties in the BG-form than in the B-form. Intermolecular interactions to be considered in the present system are the π - π interaction between the anthracene rings and the $\text{CF}\cdots\pi_{\text{F}}$ interaction.^{4a,13} The $\text{CF}\cdots\pi_{\text{F}}$ interaction is essentially the electrostatic interaction between negatively charged F atom and the positive π center. In the BG-form the $\text{CF}\cdots\pi_{\text{F}}$ interaction is effective to pile up anthracene moieties. The distances between the fluorine atoms at *p*-position and the centroids of the pentafluorophenyl moieties are 3.32 and 3.39 Å, which is within the acceptable distance for $\text{CF}\cdots\pi_{\text{F}}$ interaction.^{4a} Other weak interactions concerning F atoms are the $\text{F}\cdots\text{F}$ ^{13e,14} and $\text{CF}\cdots\text{H}$ ^{13e,15} interactions. The nature of $\text{F}\cdots\text{F}$ interactions is controversial. They would be rarely

observed and if present they would be weak. Rather repulsive interactions between negatively charged F atoms might take place. The $\text{CF}\cdots\text{H}$ interaction is also a weak interaction. It is well recognized that repulsive forces rather than attractive forces frequently play a key role in determining crystalline-state molecular packing. The sum of the weak attractive interactions as the above-mentioned could influence on the total molecular packing in balance with the repulsive forces.

Figure 3a and b shows characteristic conformations of **1** in polymorphs. The tilt angle of perfluorophenyl group defined as the angle (ω) between the mean plane of perfluorophenyl moiety and the plane bisecting the methylenes at the 9- and 10-positions of the anthracene moiety is different in both forms. The tilt angle of the B-form (58.6°) (Fig. 3a) is larger than that of the BG-form (39.7°) (Fig. 3b). The AM1 calculation showed that the energy minimum conformation was the one with almost 90° of ω as depicted in Figure 3c. The conformation with almost 0° of ω was calculated to be 12.2 kJ/mol less stable in ΔH than that of the energy minimum conformation. It seems that the smaller tilt angle is the key to have a better overlapping of anthracene moieties. Contrary to **1**, benzoyl derivative **2** did not show polymorphism. The single crystal X-ray analysis of **2** revealed that it possessed the syn-oriented benzoyl groups in contrast to the anti-oriented pentafluorobenzoyl groups in **1** (Fig. 4). Since the molecule possesses the syn-conformation, it is impossible to create the polymeric columnar array of the anthracene moieties, which was observed in the crystal structure of **1**. Only the adjacent anthracene moieties can stack facing each other to create a dimeric form. The distance between the centroids of the two adjacent anthracene moieties and the slipping angle is 4.92 Å and 46.8° , respectively. The degree of the overlap of anthracene moieties is similar to that of the B-form of **1**. The λ_{max} of the fluorescence of **2** is almost identical to that of the B-form of **1**. The red-shifted fluorescence of the BG-form of **1** could originate in more efficient overlap of the anthracene moieties.

To confirm that the fluorescence observed in the crystalline state is derived either from the excimer or the dimer associated in its ground state, excitation spectra of **1** and **2** in chloroform and the crystalline-state excitation spectra of the B-form, the BG-form, and **2** were examined.

It is known that the excitation spectrum of an excimer is identical to that of the corresponding monomer emission. In contrast, the red-shift can be observed in the excitation spectra of the dimer emission, although both emissions are identical. The excitation spectrum of **2** in chloroform was almost identical to that of **1** (Fig. 5). They are the excitation spectra for the monomer emission. In contrast, the excitation spectra of the B- and BG-forms and **2** in the crystalline state showed red-shifted spectra (Fig. 5). The results indicate that the dimeric forms of the B- and BG-forms and **2** associated in the ground state emit the fluorescence corresponding to the dimer emissions in the crystalline state. The excitation spectrum of the BG-form is slightly red-shifted than that of the B-form. This could be caused by the better overlapping of the anthracene π -planes, which brings about the longer wavelength of the fluorescence of the BG-form in the crystalline state.

We have found that the $\text{CF}\cdots\pi_{\text{F}}$ interaction plays a subtle role in polymorphs of the perfluorophenyl derivative. This slipping type interaction promotes the stacking of anthracene moieties resulting in a fabrication of aromatic columnar arrays.

Crystallographic data of the structural analyses have been deposited with the Cambridge Crystallographic Data Centre, CCDC No. 648280 for B-form of **1**, No. 648281 for BG-form of **1**, and No. 648282 for **2**. Copies of this information can be obtained free of charge from The Director, CCDC, 12 Union Road, Cambridge, CB21EZ, UK (fax: +44 1223 336033; e-mail deposit@ccdc.cam.ac.uk or web: <http://www.ccdc.cam.ac.uk>).

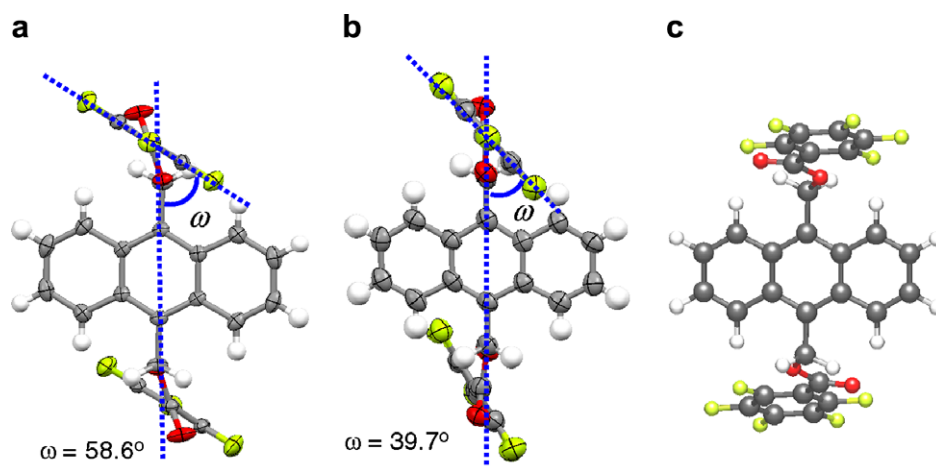


Figure 3. The tilt angle (ω) of the perfluorophenyl moiety in the B-form (a) and the BG-form (b). The energy minimum conformation of **1** calculated by AM1 (c).

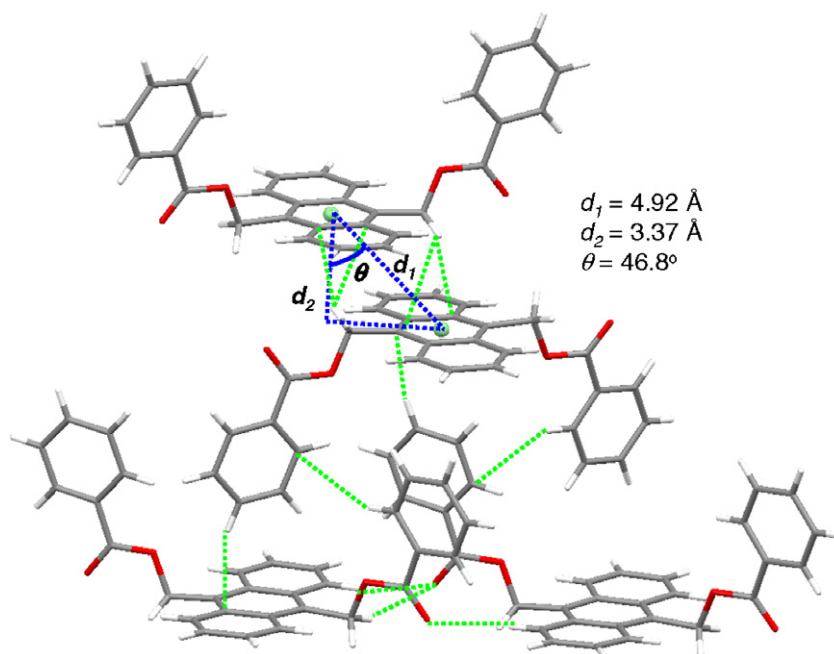


Figure 4. Packing structure of **2** showing the short contacts indicating CH/ π and C=O...H interactions. d_1 : the distance between the centroids of anthracene moieties; d_2 : the distance between the two mean anthracene planes; θ : the slippage angle.

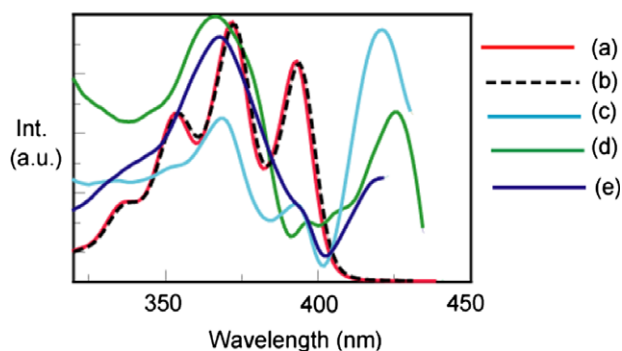


Figure 5. Normalized excitation spectra of **1** in chloroform; λ_{em} 448 nm (a), **2** in chloroform; λ_{em} 448 nm (b), the B-form in crystalline state λ_{em} 458 nm (c), the BG-form in the crystalline state; λ_{em} 485 nm (d), and **2** in the crystalline state; λ_{em} 458 nm (e).

Acknowledgement

This work was partly supported by a Grant-in-Aid for Scientific Research (C) (No. 19550031) from the Japan Society for the Promotion of Science.

Supplementary data

Supplementary data (NMR and ORTEP of **1** and **2**) associated with this article can be found, in the online version, at doi:10.1016/j.tetlet.2007.11.024.

References and notes

- (a) Moulton, B.; Zaworotko, M. J. *Chem. Rev.* **2001**, *101*, 1629–1658; (b) Desiraju, G. R. *Acc. Chem. Res.* **2002**, *35*, 565–573; (c) Hollingsworth, M. D. *Science* **2002**, *295*, 2410–2413; (d) Braga, D. *Chem. Commun.* **2003**, 2751–2754; (e) Braga, D.; Branner, J.; Champness, N. R. *Cryst. Eng. Commun.* **2005**, *7*, 1–19; (f) *Frontiers in Crystal Engineering*; Tiekink, E. R. T., Vittal, J. J., Eds.; John Wiley & Sons: Chichester, England, 2006.
- (a) Mutai, T.; Satou, H.; Araki, K. *Nat. Mater.* **2005**, *4*, 685–687; (b) Dong, Y.; Lam, J. W. Y.; Qin, A.; Li, Z.; Sun, J.; Sung, H. H.-Y.; Williams, I. D.; Tang, B. Z. *Chem. Commun.* **2007**, 40–42; (c) Sagara, Y.; Mutai, T.; Yoshikiawa, I.; Araki, K. *J. Am. Chem. Soc.* **2007**, *129*, 1520–1521.
- (a) Nishio, M.; Umesaza, Y.; Hirota, M.; Takeuchi, Y. *Tetrahedron* **1995**, *51*, 8665–8701; (b) Nishio, M.; Hirota, M.; Umezawa, Y. *The CH/ π Interaction*; Wiley-VCH: New York, 1998.
- (a) Prasanna, M. D.; Row, T. N. G. *Cryst. Eng.* **2000**, *3*, 135–154; (b) Rahman, A. N. M. M.; Bishop, R.; Craig, D. C.; Scudder, M. L. *Org. Biomol. Chem.* **2004**, *2*, 175–182; (c) Adams, H.; Cockoft, S. L.; Guardigli, C.; Hunter, C. A.; Lawson, K. R.; Perkins, J.; Spey, S. E.; Urch, C. J.; Ford, R. *ChemBioChem* **2004**, *5*, 657–665; (d) Swierczynski, D.; Luboradzki, R.; Dologons, G.; Lipkowski, J.; Schneider, H.-S. *Eur. J. Org. Chem.* **2005**, 1172–1177.
- (a) Foster, R. *J. Phys. Chem.* **1980**, *84*, 2135–2141; (b) Hunter, C. A.; Sanders, J. K. M. *J. Am. Chem. Soc.* **1990**, *112*, 5525–5534; (c) Tsuzuki, S.; Honda, K.; Uchimaru, T.; Mikami, M.; Tanabe, K. *J. Am. Chem. Soc.* **2002**, *124*, 104–112.
- (a) Mizobe, Y.; Tohnai, N.; Miyata, M.; Hasegawa, Y. *Chem. Commun.* **2005**, 1839–1841; (b) Mizobe, Y.; Ito, H.; Hisaki, I.; Miyata, M.; Hasegawa, Y.; Tohnai, N. *Chem. Commun.* **2006**, 2126–2128.
- (a) Mizobe, Y.; Miyata, M.; Hisaki, I.; Hasegawa, Y.; Tohnai, N. *Org. Lett.* **2006**, *8*, 4295–4298; (b) Mizobe, Y.; Hinoue, T.; Miyata, M.; Hisaki, I.; Hasegawa, Y.; Tohnai, N. *Bull. Chem. Soc. Jpn.* **2007**, *80*, 1162–1172.
- (a) Dong, Y.; Lam, J. W. Y.; Li, Z.; Qin, A.; Tong, H.; Dong, Y.; Fengand, X.; Tang, B. Z. *J. Inorg. Organomet.*

- Polym. Mater.* **2005**, *15*, 287–291; (b) Zhang, H.; Zhang, Z.; Ye, K.; Zhang, J.; Wang, Y. *Adv. Mater.* **2006**, *18*, 2369–2372; (c) Dong, Y.; Lam, J. W. Y.; Qin, A.; Sun, J.; Liu, J.; Li, Z.; Sun, J.; Sung, H. H. Y.; Williams, I. D.; Kwok, H. S.; Tang, B. Z. *Chem. Commun.* **2007**, 3255–3257.
9. **Compound 1**: mp 222–225 °C (B-form; recrystallized from ethyl acetate) and 221–222 °C (BG-form; recrystallized from ethyl acetate pervaded with hexane vapor). IR (KBr) 1735 cm⁻¹; UV–vis (CHCl₃) λ_{max} (ε_{max}) 340 (5870), 357 (10,400), 376 (15,400), 397 nm (15,700); ¹H NMR (500 MHz, CDCl₃) δ 8.44 (m, 4H), 7.66 (m, 4H), 6.45 (s, 4H); ¹³C NMR (125.65 MHz, CDCl₃) δ 61.06, 107.90, 124.46, 126.81, 127.69, 130.86, 137.66 (d, J_{CF} = 255 Hz), 143.36 (d, J_{CF} = 273 Hz), 145.49 (d, J_{CF} = 261 Hz), 159.22; MS (FAB) m/z 626 (M⁺). Anal. Calcd for C₃₀H₁₂F₁₀O₄; C, 57.52; H, 1.93. Found: C, 57.23; H, 1.63. *Crystal data for B-form*: monoclinic, P2₁/n, a = 15.0849 (7) Å, b = 5.8393 (3) Å, c = 28.8399 (13) Å, α = 90, β = 104.4120 (10), γ = 90, V = 2460.4 (2) Å³, Z = 4, D_c = 1.691 Mg m⁻³, T = 150 K, μ = 0.162 mm⁻¹, GOF on F² = 1.060, R₁ = 0.0377, wR₂ = 0.0919 ([I > 2σ(I)]). *Crystal data for BG-form*: Orthorhombic, Pca2₁, a = 24.824(12) Å, b = 4.252(2) Å, c = 22.746(11) Å, α = 90, β = 90, γ = 90, V = 2401(2) Å³, Z = 4, D_c = 1.733 Mg m⁻³, T = 90 K, μ = 0.166 mm⁻¹, GOF on F² = 1.041, R₁ = 0.0908, wR₂ = 0.2187 ([I > 2σ(I)]).
10. **Compound 2**: mp 250–253 °C (recrystallized from ethyl acetate). IR (KBr) 1706 cm⁻¹; UV–vis (CHCl₃) λ_{max} (ε_{max}) 339 (3900), 356 (8500), 375 (14,100), 396 nm (14,300); ¹H NMR (500 MHz, CDCl₃): δ 8.52 (m, 4H), 8.00 (dd, J = 8.2 Hz, 4H), 7.62 (m, 4H), 7.49 (t, J = 7.3 Hz, 4H), 7.35 (t, J = 7.9 Hz, 4H), 6.42 (s, 4H); ¹³C NMR (125.65 MHz, CDCl₃): δ 59.38, 124.77, 126.44, 128.34, 128.81, 129.79, 129.92, 130.94, 133.07, 166.71; MS (FAB) m/z 446 (M⁺). Anal. Calcd for C₃₀H₂₂O₄; C, 80.70; H, 4.97. Found: C, 80.97; H, 4.82. *Crystallographic data for 2*, monoclinic, P2₁/n, a = 13.1263(19) Å, b = 10.6744(16) Å, c = 16.896(2) Å, α = 90, β = 10.250(2), γ = 90, V = 2460.4 (2) Å³, Z = 4, D_c = 1.335 Mg m⁻³, T = 150 K, μ = 0.088 mm⁻¹, GOF on F² = 0.972, R₁ = 0.0481, wR₂ = 0.1041 ([I > 2σ(I)]).
11. (a) Hayashi, T.; Mataga, M.; Sakata, Y.; Misumi, S.; Morita, M.; Tanaka, J. *J. Am. Chem. Soc.* **1976**, *98*, 5910–5913; (b) Karatsu, T.; Shibata, T.; Nishigaki, A.; Kitamura, A.; Hatanaka, Y.; Nishimura, Y.; Sato, S.; Yamazaki, I. *J. Phys. Chem. B* **2003**, *107*, 12184–12191.
12. (a) Becker, H.-D.; Sandras, K.; Skelton, B. W.; White, B. A. H. *J. Phys. Chem.* **1981**, *85*, 2930–2933; (b) Endo, K.; Ezuhara, T.; Koyanagi, M.; Masuda, H.; Aoyama, Y. *J. Am. Chem. Soc.* **1997**, *119*, 499–505; (c) Ihmels, H.; Leusser, D.; Pfeiffer, M.; Stalke, D. *Tetrahedron* **2000**, *56*, 6867–6875; (d) Amicangelo, J. C.; Leenstra, W. R. *J. Am. Chem. Soc.* **2003**, *125*, 14698–14699; (e) Kwon, O.-H.; Yu, H.; Jang, D.-J. *J. Phys. Chem. B* **2004**, *108*, 3970–3974; (f) Kaanumalle, L. S.; Gibb, C. L. D.; Gibb, B. C.; Ramamurthy, V. *J. Am. Chem. Soc.* **2005**, *127*, 3674–3675; (g) Masu, H.; Mizutani, I.; Ono, Y.; Kishikawa, K.; Azumaya, I.; Yamaguchi, K.; Kohmoto, S. *Cryst. Growth Des.* **2006**, *6*, 2086–2091.
13. (a) Kim, C.-Y.; Chandva, P. P.; Jain, A.; Christianson, D. W. *J. Am. Chem. Soc.* **2001**, *123*, 9620–9627; (b) Adams, M.; Cowley, A. R.; Dubberley, S. R.; Sealey, A. J.; Skinner, M. E. G.; Mountford, P. *Chem. Commun.* **2001**, 2738–2739; (c) Liu, J.; Murray, E. M.; Young, V. G., Jr. *Chem. Commun.* **2003**, 1904–1905; (d) Caronna, T.; Liantonio, R.; Logothetis, T. A.; Metranaolo, P.; Pilati, T.; Resnati, G. *J. Am. Chem. Soc.* **2004**, *126*, 4500–4501; (e) Reichenbacher, K.; Suss, H. I.; Hulliger, J. *Chem. Soc. Rev.* **2005**, *34*, 22–30.
14. (a) Ramasubbu, N.; Parthasarathy, R.; Murray-Rust, P. *J. Am. Chem. Soc.* **1986**, *108*, 4308–4314; (b) Pedireddi, V. R.; Reddy, V. R.; Goud, B. S.; Craig, D. C.; Rae, A. D.; Desiraju, R. G. *J. Chem. Soc., Perkin Trans. 2* **1994**, 2353–2360.
15. Howard, J. A. K.; Hoy, V. J.; O'Hagan, D.; Smith, G. T. *Tetrahedron* **1996**, *52*, 12613–12622.